Formation of dislocations and hardening of LiF under high-dose irradiation with 5–21 MeV ^{12}C ions

R. Zabels[1] · I. Manika[1] · K. Schwartz[2] · J. Maniks[1] · A. Dauletbekova[3] · R. Grants[1] · M. Baizhumanov[3] · M. Zdorovets[4]

Abstract The emergence of dislocations and hardening of LiF crystals irradiated to high doses with ^{12}C ions have been investigated using chemical etching, AFM, nanoin-dentation, and thermal annealing. At fluences ensuring the overlapping of tracks ($\Phi \geq 6 \times 10^{11}$ ions/cm^2), the formation of dislocation-rich structure and ion-induced hardening is observed. High-fluence (10^{-15} ions/cm^2) irradiation with ^{12}C ions causes accumulation of extended defects and induces hardening comparable to that reached by heavy ions despite of large differences in ion mass, energy, energy loss, and track morphology. The depth profiles of hardness indicate on a notable contribution of elastic collision mechanism (nuclear loss) in the damage production and hardening. The effect manifests at the end part of the ion range and becomes significant at high fluences ($\geq 10^{14}$ ions/cm^2).

1 Introduction

Beams of swift heavy ions (SHI) have been shown to have a potential for a modification of surface and bulk properties including formation of nanostructures, amorphization, interfacial mixing, phase transitions, hardening, and other effects in various materials [1, 2].

In the studies of swift ion-induced damage, LiF crystals play an important role due to their high-radiation sensitivity and the significance for various applications (color-center lasers, dosimeters, etc.) [3–5]. In contrast to many insulators, LiF does not amorphize even under a high dose of irradiation. This property is characteristic for materials with a strong ionic bonding. Previous studies have shown remarkable SHI-induced changes of structure, optical, mechanical, and other properties in LiF [2–9]. At high-fluence irradiations, an accumulation of extended defects (dislocation loops and other aggregates of defects), nanostructuring, and substantial hardening were observed.

At comparable fluences, light ions create less pronounced changes in the structure and properties [5–7]. A difference in the damage produced by heavy and light ions manifests already in the structure of individual tracks. In LiF, high-energy heavy ions exhibiting electronic energy loss above the threshold of 10 keV/nm produce complex tracks consisting of core region (radius about 1.5–2 nm) composed of a continuous trail of small defect clusters and a much larger (tens of nm) surrounding halo region-containing color centers and their counterparts [3]. Such tracks just like dislocations are chemically etchable. In contrast, light ions in their trajectory create only the halo of color centers. The radius of the halo of light ions is markedly lower than that of heavy ions [3, 5].

However, previous studies have shown that in the ion-induced modification of the structure and micro-mechanical properties, the increase of the irradiation dose (fluence) can partially compensate the difference in the ion mass, energy, and energy loss. For instance, a strong hardening, forma-tion of dislocation-rich structures and even nanostructuring has been achieved in LiF after irradiation to high fluences

*\ R. Zabels
\ rzabels@gmail.com

1\ Institute of Solid State Physics, University of Latvia, 8 Kengaraga str., Riga 1063, Latvia

2\ GSI Helmholtzzentrum für Schwerionenforschung, 1 Planckstr., 64291 Darmstadt, Germany

3\ L.N. Gumilyov Eurasian National University, 5 Munaitpassov Str., 010008 Astana, Kazakhstan

4\ Institute of Nuclear Physics, 1 Ibragimov Str., 050032 Almaty, Kazakhstan

(up to 5 × 10^{14} ions/cm^2) with 5–10 MeV gold ions, the energy loss for which (<4 keV/nm) is below the threshold for core damage [9]. It is of interest to elucidate weather similar damage and modifications of properties can be achieved by a high-fluence irradiation with light ions. The tendency of aggregation of radiation defects in LiF at high-fluence irradiation of ^{12}C ions has been reported in [5, 10].

In this study, the changes of the structure and micro-mechanical properties in LiF crystals irradiated to high doses with light ^{12}C ions have been investigated. The atten-tion has been devoted to the role of the fluence, energy loss, and track overlapping in the creation of dislocations as well as on the thermal resistance of structures created under severe irradiation. Unfortunately, the most informa-tive TEM technique cannot be applied for dislocation stud-ies due to a high-radiation sensitivity of LiF crystals. The dislocation structure was revealed by selective chemical etching [11–13]. The evolution of damage was character-ized also by nanoindentation, which is highly sensitive to dislocations and other aggregates of radiation defects [7, 9].

2 Experimental

For the irradiation experiments, high-purity LiF crystals which have been grown from a melt in an inert atmos-phere by the Stockbarger method (Optical institute, St. Petersburg, Russia) were used. The dislocation density in these crystals was determined to be around 10-^{3}–10^4 cm^{-2}. The crystals were transparent in the spectral range from 190–1100 nm with the absorption cefficient μ = 0.05 cm^{-1}. Small (5 × 5–10 × 10 mm) LiF platelets (thickness ≤1 mm) were prepared by cleaving from larger LiF single-crystal blocks.

Irradiation was performed at the cyclotron DC-60 (Astana, Kazakhstan) using 4.8, 12, and 21 MeV ^{12}C ions at fluences (Φ) from 5 × 10^{10} to -10^{15} ions/cm^2 determined with an accuracy of 10% (Table 1). For all irradiations, the density of the ion current was kept at 10 nA/cm^2. The temperature of samples during irradiation did not rise above 360 K. All irradiations were performed under nor-mal incidence of the ions to the (100) face of crystals. The ion range and energy loss was calculated using SRIM 2013 freeware package [14].

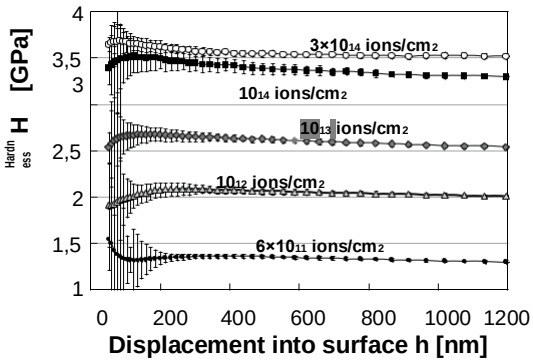

Fig. 1 Hardness on the frontal surface as a function of indentation depth for LiF irradiated with 21 MeV ^{12}C ions at different fluences. The hardness for an unirradiated crystal at the indentation depth of 1.5 μm is 1.3 GPa

Nanoindentation was performed by an instrumented indentation unit G200 (Agilent, USA) using a Berkovich diamond tip (tip curvature <20 nm) in ambient air at room temperature. The strain rate was 0.05 s^{-1}.The area func-tion of the indenter tip was calibrated using a Corning glass reference sample. For the calculation of hardness and Young's modulus, the Oliver–Pharr model was used [15]. The results have been averaged from at least 10 individual measurements, which at a given surface roughness provide adequate statistics. The values of hardness, modulus, and standard deviation of measurements were calculated from experimentally obtained loading–unloading curves using the MTS TestWorks 4 software.

For the characterization of the induced damage along the ion trajectory irradiated platelets of LiF were cleaved along the direction of the ion beam thus revealing fresh surfaces suitable for indentation. In the following text, these surfaces will be regarded as profile surfaces in order to distinguish them from the irradiated or frontal surfaces which are oriented normally to the ion beam. For the prob-ing of hardness on profile surfaces, a basic measurement technique with an indenter penetration depth of 150 nm was utilized. The measurement errors were in the range of 0.04–0.05 GPa. For the hardness measurements on the irradiated frontal surface, a continuous stiffness technique was employed. The variation of errors with indentation depth is shown in Fig. 1. The main source of errors is the

Table 1 Irradiation parameters

Ion /charge	Ion energy E_{ion} (MeV)	Fluence ions/cm^2	Calculated ion range R (μm)	E_{ion}/R (keV/nm)	Max. irrad. dose (at 10^{15} ions/cm^2) (MGy)
$^{12}C^{+1}$	4.8	5 × 10^{10}–10^{15}	4.19	1.15	695
$^{12}C^{+2}$	12	5 × 10^{10}–10^{15}	8.74	1.35	833
$^{12}C^{+3}$	21	5 × 10^{10}–10^{15}	16.0	1.31	797

surface roughness which in our samples includes cleavage steps and other surface irregularities. The errors related to influence of vibrations and drift processes in the measurement system were minimized using recommended testing procedures.

The distance between the irradiated surface and an indentation imprint on a profile surface was determined by means of optical microscopy (Eclipse L150, Nikon) with an accuracy of 1.5 μm.

In some experiments, the indentation hardness was supplemented with the dislocation mobility technique, based on the measurements of the size of dislocation rosettes around indentations [16]. In order to distinguish between the hardness and dislocation mobility data, the latter were performed using Vickers indenter.

The dislocation structure in irradiated LiF samples was revealed by a short-time (~1 s) selective chemical etching in a saturated aqueous -$FeCl_3$ solution and a subsequent imaging by atomic force microscope (AFM) CPII (Veeco, USA) in the tapping-mode.

Thermal annealing experiments were performed on samples irradiated with 21 MeV ^{12}C ions to fluence of 10^{15} ions/cm^2 in air atmosphere with the duration of thermal exposure of 10 min.

Measurements of optical absorption were performed using UV/VIS spectrometer Specord M250 (Analytik Jena) in the spectral range 190–700 nm. All absorption measurements were carried out against a non-irradiated LiF crystal.

3 Results

3.1 Ion- induced hardening on frontal and profile surfaces

Nanoindentation tests on the frontal surface oriented normally to the ion beam showed a remarkable hardening effect in LiF crystals irradiated with 4.8, 12, and 21 MeV ^{12}C ions. The hardness vs. indentation depth curves for sample irradiated with 21 MeV ions at different fluences are shown in Fig. 1. The hardness values after irradiation to fluences 5×10^{10}, 10^{11}, and 6×10^{11} ions/cm^2 within the experimental errors coincide with the hardness of the unirradiated crystal. Dislocation mobility measurements also did not show any effect. The hardening effect appears at fluences above 6×10^{11} ions/cm^2, increases with the fluence, and reaches saturation around 140% at fluences above 6×10^{13} ions/cm^2. A slight increase of the hardness with decreasing the indentation depth can be related to the indentation size effect [17] and partially also to irradiation-induced surface modifications [18].

The nanoindentation results on the frontal surface also show an ion-induced increase of Young's modulus. However, the magnitude of the effect is comparatively small (about 18%) and lies in the range of commonly observed modulus data for LiF which has been exposed to various kinds of irradiations.

In order to characterize the damage along the ion path, the measurements of hardness were performed on profile surfaces. Comparatively small indents (depth 150 nm) were used to ensure a reasonably large number of data points with still acceptable errors. Results presented in Fig. 2a, b show the evolution of hardness on cross-section of sam-ples irradiated with 12 and 21 MeV ^{12}C ions at different fluences. At fluences 5×10^{10} and $\sim 10^{11}$ ions/cm^2, no detect-able hardening was observed. At fluences of 3×10^{11} and 6×10^{11} ions/cm^2, the hardening on profile surface appeared only in the region of Bragg's maximum. At higher fluences, the effect of hardening increases and its variation along the ion path approximately follows the change of the electronic energy loss calculated by SRIM. This tendency is clearly seen in Fig. 2b.

The depth profiles of nanohardness reveal some important details of damage. A strong hardening is observed at

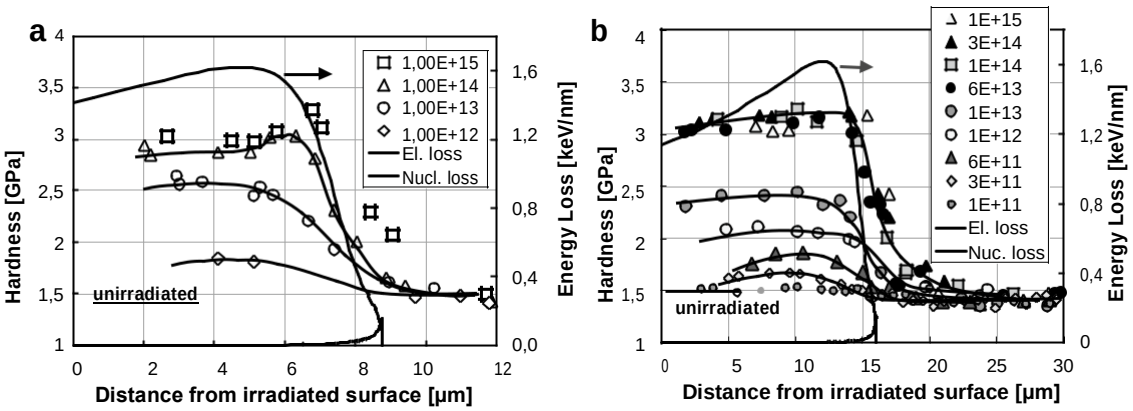

Fig. 2 The depth profiles of hardness of LiF irradiated with 12 MeV (**a**) and 21 MeV ^{12}C ions (**b**) to different fluences. For the comparison, the calculated depth profiles of electronic energy loss (*dashed line*) and nuclear loss (*solid line*) are plotted

the end of the ion range despite of the fact that the values of calculated electronic energy loss decrease to low values. At high-fluence irradiation, the region of maximum harden-ing is extended toward the end of the ion range, where the nuclear energy loss displays a maximum (Figs. 2, 3). Simi-lar effect was observed earlier in LiF irradiated to high flu-ences with MeV energy ^{131}Xe ions and in MgO irradiated with ^{84}Kr and ^{14}N ions. It was explained by the contribution of the elastic collision mechanism (nuclear stopping) in the ion-induced damage [19, 20]. We can conclude that under conditions of severe irradiation light, ^{12}C ions are also able to produce a strong damage and hardening via the elastic collision mechanism. The effect manifests at high fluences in a narrow zone close to the end of the ion range.

Another peculiarity is the upper limit of hardening. The hardness values at the highest fluences for all applied ion energies saturate approaching nearly the same values (~3.2 GPa) and become almost independent of the ion energy, energy loss, and fluence. First, this limit is reached at the Bragg's maximum and with a further increase of flu-ence the zone of maximum hardening broadens toward the incoming side of ions. The dislocation mobility in heavily irradiated samples is strongly suppressed, and the deforma-tion zone at indentation becomes localized in shear bands close to the indents (Fig. 4). Such limit of hardening in LiF was observed in earlier studies for different projectiles [5, 21]. The saturation of the ion-induced hardening is ascribed mainly to the exhaustion of the dislocation mechanism of the plastic deformation and activation of a non-dislocation mechanism based on local atomic rearrangements. Such mechanism requires high applied indentation pressures. It should be noted that the pressure over indents on heavily irradiated LiF by a factor of two exceeds that for a virgin crystal. From a methodological point of view, the hard-ness after reaching this upper limit becomes uninformative

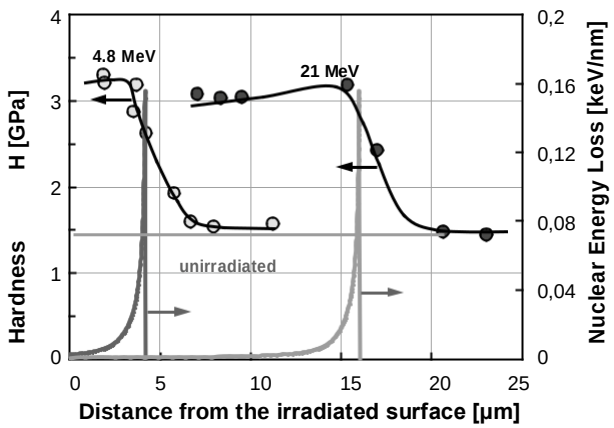

Fig. 3 The depth profiles of hardness and calculated nuclear energy loss in LiF irradiated with 4.8 and 21 MeV ^{12}C ions at fluence 10^{15} ions/cm^2

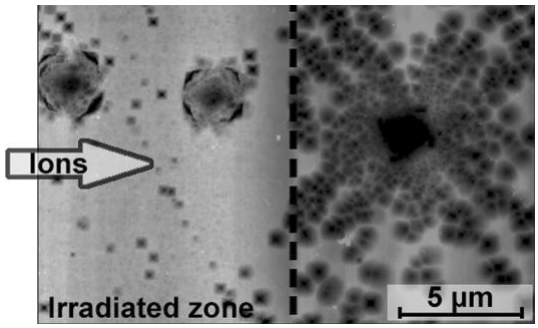

Fig. 4 AFM image of dislocation rosettes around indentations per-formed at a constant load (4.9 mN) inside the irradiated zone (on the *left*) and on the adjacent non-irradiated surface (on the *right*). *Dashed line* denotes the end of the ion range. Irradiation was performed with 21 MeV ^{12}C ions, $\Phi = 10^{14}$ ions/cm^2

about the evolution of structure and properties at a further increase of fluence.

The results show a slight increase of hardness also in the adjacent non-irradiated zone up to 3 μm beyond the ion range (Figs. 2, 3). The effects of color-center forma-tion and hardening beyond the range of swift ^{12}C ions were observed earlier [7, 22] and have attracted attention in the recent studies [23]. However, the observed enlargement of the hardened zone, which manifests at high fluences, in our case is small (few μm) and can be considered rather as a well-known edge effect in hardness tests caused by a defi-nite size of the deformation zone around indents. In favor of this statement is also that the coincidence of the calcu-lated ion range with the size of the damaged zone revealed by etching.

3.2 Evolution of dislocation structure revealed by chemical etching

Irradiation with light ions, which in contrast to swift heavy ions do not create etchable tracks, provides an opportunity for the study of structural damage by chemical etching directly on frontal surface. The etching on samples which were irradiated to high fluences reveals numerous etch-ing pits thus indicating the presence of defect aggregates. Based upon the following considerations, we assigned such aggregates mainly to the prismatic interstitial dislocation loops (schematically shown in Fig. 5):

1.\ Prismatic interstitial dislocation loops in alkali halide crystals including LiF have been observed by in-situ TEM studies under irradiation with electron beam [24, 25]. Also swift ions in solids induce ionization events along the ion path and create δ-electrons with a broad spectrum of kinetic energies;

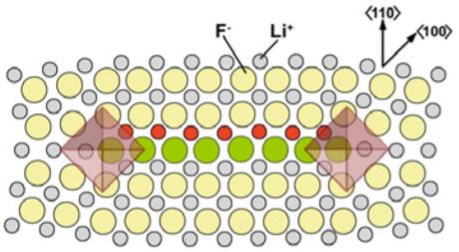

Fig. 5 Schematic of a cross-section of perfect interstitial disloca-tion loop in LiF with a (110) *slip plane* and Burgers vector *a*/2 [110]. *Large circles* denote anions (F^-) and *smaller circles* cations -(Li^+). Perfect dislocation is constructed by inserting two extra-planes of ions (*filled circles*). Chemical etching at intersection points of the loop line with surface reveals two etching pits (marked by *overlaid squares*)

2.\ At room temperature irradiation, formation of alternative aggregates, e.g., colloids seems to be unlikely taking into account that *F*–centers under such conditions are practically immobile [26];

3.\ Ion-induced dislocation loops are directly observed by TEM in related ionic crystals (MgO and spinels) [27]; 4.\ It is experimentally shown that etching pits in ion-irradiated LiF belong to defect aggregates which can move under applied stress [6]. Among different kinds of defect aggregates, only dislocations have such abil-ity. The experiments were performed on LiF irradiated with 410 MeV ^{38}S ions, the energy loss of which in the major part of the range is below 5 keV/nm. Irradiated samples were subjected to indentation and then etched. The results showed the change in the layout of etchable aggregates in the stress field of indentations.

Of course, at the highest irradiation doses formation of some amount of other aggregates, such as small colloids, vacancy and fluorine bubbles could be possible even at room temperature irradiation.

Chemical etching on the frontal (001) surface reveals the first signs of defect aggregates in the form of rounded etching pits at fluences above 6×10^{11} ions/cm^2. Such pits (Fig. 6a, c) can be attributed either to nuclei of dislocations or to small (5–7 nm) dislocation loops. Clearly recognizable pyramidal etching pits typical for dislocations appear after irradiation to fluences above 10^{12} ions/cm^2 (Fig. 6b). The uniform orientation of etching pits with sides along <100> direction speaks about maintained single-crystal-line state of irradiated samples. The density of dislocations on the irradiated surface increases with the fluence and at 10^{14} ions/cm^2 reaches around 1.5×10^{10} cm^{-2}. At the maximum fluence (10^{15} ions/cm^2), the resolution of the disloca-tion structure deteriorates due to decrease of the selectivity of etching and superimposition of numerous small etching pits.

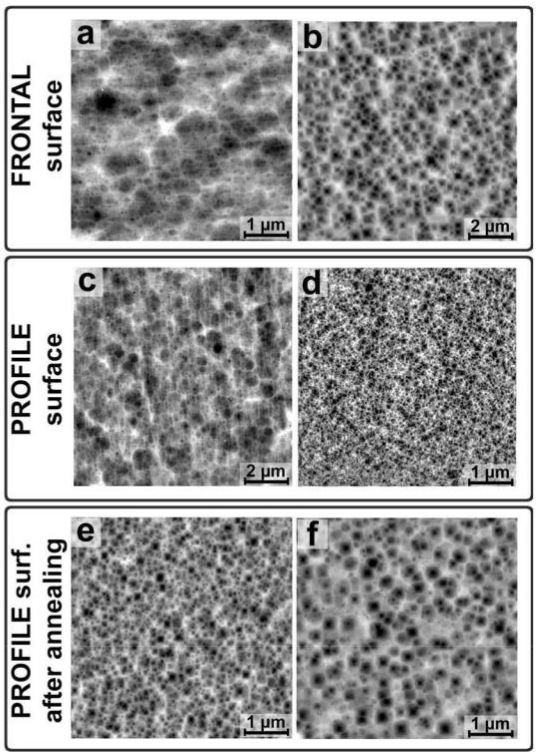

Fig. 6 AFM images of dislocation structure in LiF exposed to irradiation with 21 MeV ^{12}C ions at different fluences: **a** and **b** frontal surface at $\Phi = 10^{12}$ and $\Phi = 10^{13}$ ions/cm^2, correspondingly, **c** and **d**—profile surface at $\Phi = 10^{12}$ and $\Phi = 10^{15}$ ions/cm^2, correspondingly. Images **e** and **f** show profile surfaces, irradiated at $\Phi = 10^{15}$ ions/cm^2, and annealed at 590 and 680 K, correspondingly

In the analysis of the obtained dislocation structures, following points should be taken into account. First, when such loop intersects the surface under investigation, the etching reveals a mutually related pair of etching pits [6]. During chemical etching, pits of the smallest loops might merge forming almost square shaped or slightly elongated rectangular figures. Larger loops can form well separated pairs of etching pits. The distance between their centers approximately characterizes the size of the loop. Etch-ing pits and their pairs can be seen in Fig. 6b. Second, the shape of etching pits depends on the impurities and radiation defects that are segregated on dislocations. It is commonly observed that fresh dislocations free from atmospheres of impurities or radiation defects in LiF etch as square-based pyramids, while those with atmospheres etch rounded [12, 13].

At moderate fluences, the size of observed pits var-ies along the ion trajectory being smaller and rounded in the incoming and end parts of the range compared to that around the Bragg's maximum. However, at the highest fluences, we can see densely packed small pits all over the range (Fig. 6d).

The comparison of results of dislocation etching and nanoindentation allows us to conclude that ion-induced hardening and formation of dislocation-rich structures in LiF crystals irradiated with 4.8–21 MeV ^{12}C ions appears at fluences $\Phi > 6 \times 10^{11}$ ions/cm^2. The resolution of the selective chemical etching technique was insufficient to answer the question, whereas dislocations or their nuclei are formed in individual far standing tracks of ^{12}C ions. Further effort for solving this task is required.

3.3 Thermal recovery of structure produced by severe irradiation with ^{12}C ions

The recovery behavior of optical absorbance, structure, and hardness under annealing has been studied in LiF samples irradiated with 21 MeV ^{12}C ions at fluence 10-^{15} ions/cm^2.

The optical absorption spectra at different stages of annealing are presented in Fig. 7. Before annealing irradiated samples show an absorption spectrum typical for irradiated LiF in which the strongest absorption bands at 245 and 445 nm belong to F and F_2 centers, respectively. At the first step of annealing (590 K), the 245 nm absorption band disappears, while the 445 nm band is reduced and broadened. Such transformation is related to annealing of single defects as well as to their aggregation and formation of Li colloids [4, 7]. The absorption band at 275 nm typical for Mg impurity colloids is absent for the investigated high-purity crystals. During further annealing (680 K), the absorption maximum is reduced even more due to decomposition of colloids and shifted toward higher wavelength that according to [4] confirms the change in colloid size. The absorption bands in spectra disappear after annealing above 740 K.

The annealing of irradiated samples strongly improved the selectivity of etching. A better resolution and contrast as well as disappearance of the smallest etching pits was reached already after annealing at 590 K (Fig. 6e). The annealing at 680 K leads to a decrease of the density of etching pits to 10-^{9} cm^{-2} (Fig. 6f). A gradual reduction of the density of defects continues under annealing at higher temperatures and a full recovery of the structure is reached after annealing at $T \geq 810$ K. Uniform orientation of etching pits of dislocations gives evidence for single-crystalline state of annealed samples.

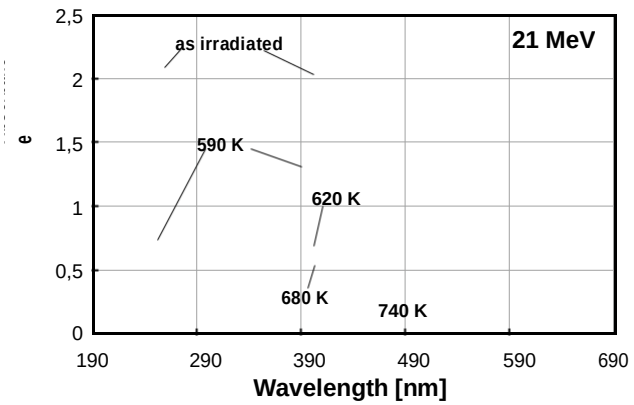

Fig. 7 Absorption spectra of irradiated LiF before and after annealing at different temperatures. Irradiation performed with 21 MeV ^{12}C ions to fluence of 10-^{15} ions/cm^2

The obtained optical absorption data for annealed samples confirm the presence of lithium colloids. However, we were not able to recognize colloids in the etching images at different stages of annealing. Such peculiarity could be related to specifics of colloid formation in dislocation-rich crystals. As shown in [28], formation of intrinsic colloids in LiF can occur in the vicinity of dislocations as preferen-tial sites for metal precipitates. Our annealing experiments were performed on heavily irradiated dislocation-rich crystals and growth of complex defect aggregates seems possible at certain stage of annealing.

The depth profiles of hardness after annealing of irradiated crystals in the range of 593–740 K are presented in Fig. 8a. The recovery of hardness begins at temperatures above 530 K and completes under annealing at about 810 K. The results show a faster recovery of the structure and hardness in the incoming and the tail sides of the range as compared to the region of Bragg's maximum (Fig. 8b). Besides, the maximum of residual hardening at temperatures above 680 K shifts to the center of the irradiated zone. Possible reasons of a non-uniform recovery along the ion path could be the stronger damage at the Bragg maximum and a sink role of the free surface and interface between irradiated and unirradiated crystal for defects formed by thermal decomposition of dislocations and other extended defects. For the analysis of recovery processes in dislocation and colloid subsystems, a further study of the recovery kinetics at annealing times sufficiently long for achieving the equilibrium conditions of recovery is required.

4 Discussion

The obtained results show that severe irradiation of LiF crystals with light ^{12}C ions in the energy range of 4.8–21 MeV creates strong structural damage and causes hardening approaching that reached by irradiation with high-energy heavy ions, despite of large differences in the ion mass, energy, energy loss, and track morphology. A comparable hardening with ^{12}C ions is reached at ~2 orders of magnitude higher fluences than with heavy ions (^{197}Au, ^{209}Bi, ^{131}Xe, etc.) exhibiting stopping power >10 keV/nm.

Furthermore, for ^{12}C ions, some peculiarities in the damage behavior have been observed:

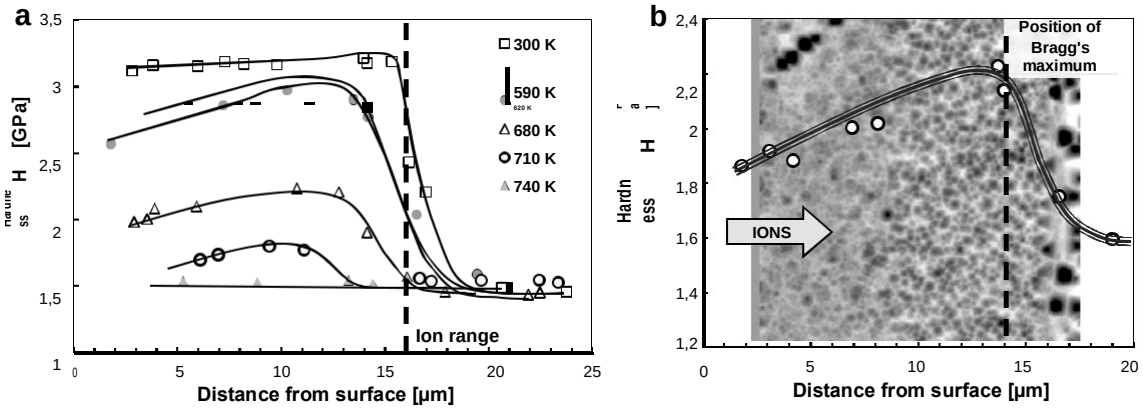

Fig. 8 Depth profiles of hardness after annealing at different temperatures for LiF irradiated with 21 MeV ^{12}C ions to fluence of 10^{15} ions/cm^2 (**a**) and the AFM image of an etched profile surface of LiF after annealing at 680 K with an overlaid hardness profile, irradiation with 21 MeV ^{12}C ions to fluence of 3×10^{14} ions/cm^2 (**b**)

- Etching experiments on samples irradiated with ^{12}C ions reveal only a dislocation-rich structure even after applying the maximum fluences. In contrast, at high-flu-ence irradiation with heavy ions, the dislocation struc-ture at high doses becomes ordered and transforms into a mosaic-type nanostructure [7].
- For ^{12}C ions, a notable contribution of elastic collision mechanism (nuclear loss) in the damage production and hardening is observed. The effect manifests at high fluences ($\geq 10^{14}$ ions/cm^2) at the end part of the ion range.

Individual tracks of ^{12}C ions are weak obstacles for indentation-induced dislocations. Neither hardness tests, nor measurements of dislocation mobility as a more sensitive method reveal the hardening effect in samples irradiated to lower fluences ($\leq 5\times 10^{10}$ ions/cm^2) when mainly individual tracks are formed (see Sect. 3.1). A similar behavior is observed for ^{58}Ni, ^{36}S, and other comparatively light ions with electronic energy loss in LiF below 10 keV/ nm [16, 29].

Specifics of interaction of swift ions with solids are the discrete nature of ion impacts and localization of dam-age in tracks. The results for LiF crystals irradiated with 4.8–21 MeV ^{12}C ions show hardening effect and emer-gence of dislocations at fluences $\Phi > 6\times 10^{11}$ ions/cm^2 at which the overlapping of tracks (ions hitting pre-irra-diated areas) might become significant. The first step in appraising the role of track overlapping was the estima-tion of the surface covering with tracks as a function of fluence for 21 MeV ^{12}C ions (Fig. 9). The ratio of the irradiated area (A) to nominal area (A_0) was calculated from

$$A/A_0 = 1-\exp(-\pi r_F^2\times\Phi)$$

, where Φ is the fluence and r_F is the average radius of the ion track, which was estimated from the data of optical absorption spectroscopy [10] as $r_F = 1.6 \pm 0.3$ nm. The Poisson's law [30]:

However, the Poisson's law characterizes the evolution of irradiated area without distinguishing between individual and overlapped tracks, created at double or multiple impacts of ions. According to investigations of areal dispersion of tracks based on statistical nature of events, the probability of ion hitting pre-irradiated areas cannot be neglected even at an early stage of surface covering with tracks [31].

The formalism for calculation of track overlapping is well developed and includes fluence dependencies for probabilities of single, double, and following multiple hits at different limiting conditions [31 –33]. Therefore, we estimated the fluence dependency for (1) the probabil-ity of double hit events and for (2) the percentage of over-lapped areal fraction in double hits. The probability of

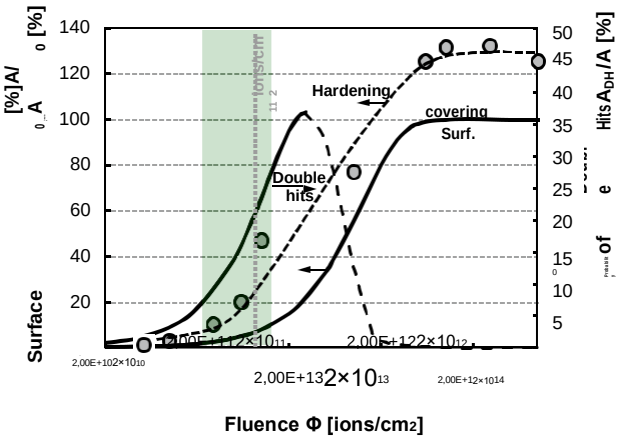

Fig. 9 The fluence dependency of hardening ($\Delta H/H_0$) on the profile surface, calculated surface covering (A/A_0) by tracks and probability of double hits (A_{DH}/A_0) (*right axis*). The hardness data were taken from Fig. 2b for 21 MeV ^{12}C ions at the Bragg's maximum. The *colored* band marks the boundaries of threshold fluences for hardening

double hit events, which showed a better correlation with the experimentally obtained hardening data, according to [32], was calculated as $P_2 = 4\Phi_{PRF}^2 \times \exp(-4\Phi_{PRF}^2)$. Here the overlapping by double impacts characterizes the probability for all events where the track of incident ion at least partly falls into the damage trail left by the previ-ous ion. The result is also presented in Fig. 9 (right axis). As seen, the curve of double hits (A_{DH}/A, %) reaches a maximum of ~36% at the fluence of 2×10^{12} ions/cm^2 after which (dashed downward slope of the curve) contribution of higher multiplicity hits becomes significant. It should be noted that at the fluence $\Phi \approx 6 \times 10^{11}$ ions/ cm^2 , for which an intense evolution of dislocation struc-ture and undeniable hardening is observed, the calculated contribution of double hits is noticeable (~20%, which corresponds to ~1.5% of nominal area A_0) . We can conclude that tracks formed in LiF by double impact of ^{12}C ions are strong obstacles for indentation -induced dislocations compared to individual tracks. A similar behavior was reported in our previous study on dislocation formation in tracks of swift heavy ions (^{238} U) where dislocation nuclei were revealed in individual far standing tracks, while intense growth of dislocations was observed for tracks in pre-irradiated areas [6]. We suggest that double impacts of ions promote the growth of dislocation loops also in the case of ^{12}C ions.

Generally, the results of the present study confirm the necessity of track overlapping in the modification of structure and mechanical properties of LiF crystals irradiated with light ^{12}C ions, electronic energy loss for which is far below 10 keV/nm. The damage by double impact of ions is considered as the initial stage of formation of stable dislocation loops at which the ion-induced hardening is initiated. The Hobb's model provides a reasonable explana-tion of the mechanism of dislocation growth [24]. Further growth and accumulation of dislocations and other aggregates of defects continues with ongoing ion impacts up to saturation stage at $\Phi \geq 10^{14}$ ions/cm^2.

In the light of the obtained results, a series of questions regarding the mechanism of dislocation formation and the damage behavior in overlapping tracks as well as property modifications under severe irradiation remain open.

Acknowledgements R. Zabels, I. Manika, J. Maniks, and R.Grants acknowledge the national project IMIS2, and A. Dauletbekova, M. Baizhumanov, and M. Zdorovets the Ministry of Education and Science of the Republic of Kazakhstan for the financial support.

References

\ 1.\ D.K. Avasthi, G.K. Mehta, *Swift Heavy Ions for Materials Engineering and Nanostructuring*. (Springer, New Delhi, 2011)
\ 2.\ P. Apel, Nucl. Instr. Meth. B **208**, 11 (2003)
\ 3.\ K. Schwartz, C. Trautmann, T. Steckenreiter, O. Greib, M. Krämer, Phys. Rev. B **58**, 11232 (1998)
\ 4.\ K. Schwartz, A.E. Volkov, M.V. Sorokin, R. Neumann, C. Traut-mann, Phys. Rev. B **82**, 144116 (2010)
\ 5.\ K. Schwartz, J. Maniks, I. Manika, Phys. Scr. **90**, 094011 (2015)
\ 6.\ R. Zabels, I. Manika, K. Schwartz, J. Maniks, R. Grants, Nucl. Instr. Meth. B **326**, 318 (2014)
\ 7.\ J. Maniks, I. Manika, R. Zabels, R. Grants, E. Tamanis, K. Schwartz, Nucl. Instr. Meth. B **282**, 81 (2012)
\ 8.\ A. Dauletbekova, J. Maniks, I. Manika, R. Zabels, A.T. Akilbe-kov, M.V. Zdorovets, Y. Bikhert, K. Schwartz, Nucl. Instr. Meth. B **286**, 56 (2012)
\ 9.\ J. Maniks, I. Manika, R. Grants, R. Zabels, K. Schwartz, M. Sorokin, R.M. Papaleo, Appl. Phys. A **104**, 1121 (2011)
10\.\ A. Dauletbekova, K. Schwartz, M.V. Sorokin, M. Baizhumanov, A. Akilbekov, M. Zdorovets, Nucl. Instr. Meth. B **359**, 53 (2015)
\11.\ J.J. Gilman, W.G. Johnston, J. Appl. Phys. **29**, 877 (1958)
\12.\ J.J. Gilman, W.G. Johnston, G.W. Sears, J. Appl. Phys. **29**, 747 (1958)
\13.\ W.G. Johnston, J.J. Gilman, J. Appl. Phys. **30**, 129 (1959)
14\.\ J.F. Ziegler, J.P. Biersack, U. Littmark, *The Stopping And Range Of Ions In Solids* (Pergamon Press, New York, 1985)
\15.\ W.C. Oliver, G.M. Pharr, J. Mater. Res. **7**, 1564 (1992)
\16.\ I. Manika, J. Maniks, K. Schwartz, J. Phys. D Appl. Phys. **41**, 074008 (2008)
\17.\ I. Manika, J. Maniks, Acta Mater. **54**, 2049 (2006)
18\.\ H. Hijazi, H. Rothard, P. Boduch, I. Alzaher, F. Ropars, A. Cassimi, J.M. Ramillon, T. Been, B. Ban d'Etat, H. Lebius, L.S. Farenzena, E.F. da Silveira, Nucl. Instr. Meth. B **269**, 1003 (2011)
\19.\ R. Zabels, I. Manika, K. Schwartz, M. Baizhumanov, R. Grants, E. Tamanis, A. Dauletbekova, M. Zdorovets, Phys. Stat. Sol. B **253**, 1511 (2016)
20\.\ R. Zabels, I. Manika, K. Schwartz, J. Maniks, R. Grants, M. Sorokin, M. Zdorovets, Appl. Phys. A **120**, 167 (2015)
\21.\ J. Maniks, R. Zabels, I. Manika, IOP Conf. Series: Mater. Sci. Eng. **38**, 012017 (2012)
22\.\ V.R. Regel, L.I. Alekseeva, A.A. Urusovskaya, G.G. Knab, G.V. Sotserdotova, Radiat. Eff. **82**, 157 (1984)
\23.\ M.V. Sorokin, K. Schwartz, K.-O. Voss, O. Rosmej, A.E. Volkov, R. Neumann, Nucl. Instr. Meth. B **285**, 24 (2012)
\24.\ L.W. Hobbs, A.E. Hughes, D. Pooley, R. Proc. Soc. London A, **332**, 167 (1973)
\25.\ Y. Kawamata, J. Phys. Colloques **37**(C7), C7–C502 (1976)
26\.\ E.A. Kotomin, A.I. Popov, in *Radiation effects in solids*, ed. by K.E. Sickafus et al (Springer, Amsterdam, 2007), p. 153
\27.\ S.J. Zinkle, V.A. Skuratov, Nucl. Instr. Meth. B **141**, 737 (1998)
28\.\ A.T. Davidson, J.D. Comins, A.M.J. Raphuthi, A.G. Kozakiewicz, E.J. Sendezera, T.E. Derry, J. Phys.: Condens. Matter. **7**, 3211 (1995)
\29.\ I. Manika, J. Maniks, M. Toulemonde, K. Schwartz, Nucl. Instr. Meth. B **267**, 949 (2009)
30\.\ P. Thevenard, G. Guiraud, C.H.S. Dupuy, B. Delaunay, Radiat. Eff. **32**, 83 (1977)
\31.\ C. Riedel, R. Sphor, Radiat. Eff. **42**, 69 (1979)
32. R. Sphor, *Ion tracks and Microtechnology principles and applications*, K. Bethge (Ed.), (Vieweg & Sohn, Braunschweig, 1990), p. 177
\33.\ N. Ishikawa, K. Ohhara, Y. Ohta, O. Michikami, Nucl. Instr. Meth. B **268**, 3273 (2010)

Institute of Solid State Physics, University of Latvia as the Center of Excellence has received funding from the European Union's Horizon 2020 Framework Programme H2020-WIDESPREAD-01-2016-2017-TeamingPhase2 under grant agreement No. 739508, project CAMART²